analytical chemistry

pubs.acs.org/ac Article

Ultrasonic-Based Filter Aided Sample Preparation as the General Method to Sample Preparation in Proteomics

Luís B. Carvalho, José-Luis Capelo-Martínez, Carlos Lodeiro, Jacek R. Wiśniewski, and Hugo M. Santos*

Cite This: *Anal. Chem.* 2020, 92, 9164−9171 Read Online

ACCESS | Metrics & More | Article Recommendations | Supporting Information

ABSTRACT: We propose a new high-throughput ultrafast method for large-scale proteomics approaches by speeding up the classic filter aided sample preparation protocol, FASP, from overnight to 2.5 h. Thirty-six samples can be treated in 2.5 h, and the method is scalable to 96-well plate-based pipelines. After a modification of the FASP-tube, the steps of protein reduction, protein alkylation, and protein digestion of complex proteomes are done in just 5.25 min, each one under the effects of an ultrasonic field (7 cycles: 30 s on and 15 s off). The new method was compared to the standard overnight digestion FASP protocol, and no statistical differences were found for more than 92.4%, 92%, and 93.3% of the proteins identified by studying the proteome of *E. coli*, mouse brain, and mouse liver tissue samples, respectively. Furthermore, the successful relative label-free quantification of four spiked proteins in *E. coli* samples, BSA, β-lactoglobulin, α-casein, and α-lactalbumin, was achieved, using either the ultrasonic-based FASP protocol or the classic overnight one. The new US-FASP method matches the analytical minimalism rules as time, cost, sample requirement, reagent consumption, energy requirements, and production of waste products are reduced to a minimum while maintaining high sample throughput in a robust manner as all of the advantages of the filter aided sample preparation protocol are maintained.

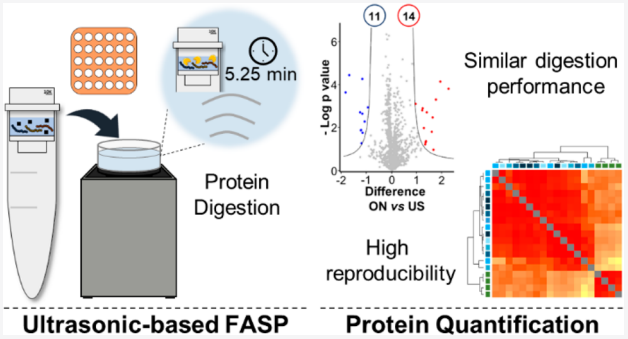

Mass spectrometry-based bottom-up protein quantification of complex proteomes relies on extensively handling and time-consuming approaches; all of them share several steps, including proteome extraction and solubilization, fractionation of the proteome (to reduce complexity), reduction and alkylation of protein disulfide bonds, and proteome digestion using enzymes.[1]

The protein digestion step is the most time-consuming in the pipeline for proteome-wide quantification, as the standard protocols often rely on overnight incubations lasting up to 18 h.[1,2] Therefore, attempts to reduce such time-consuming steps are reported in the literature. Thus, it has been demonstrated that the enzymatic digestion of proteins can be accelerated through an array of different tools, including microwave energy, infrared energy, heating, electrical fields, ultrasonic energy, and immobilized enzymes.[2,3] In this context, ultrasonic energy as a way to speed up digestion of complex proteomes for protein identification from overnight to some minutes was first reported in 2005 by Ferrer et al.[4] Subsequent developments of this methodology showed that ultrasonic energy can also accelerate from tens of minutes to some few the reduction and alkylation of protein's disulfide bonds.[5−11] Furthermore, it has been shown recently that ultrasonic energy can also be successfully applied in the format of a 96-well plate, which thus makes it possible to digest 96 samples in just 4 min.[12] As the methodology was applied for protein identification, it remains unknown if such an approach can also be applied for protein quantification by mass spectrometry.

Filter aided sample preparation (FASP) is a frequently used sample treatment method in proteomics.[13,14] The method uses ultrafiltration membrane for protein handling and isolation of clean peptide fraction. In brief, in-solution complex protein mixtures are separated from other components using an ultrafiltration device where a membrane, with a certain cutoff, is used to retain the proteome content, while allowing the removal of smaller contaminant molecules and interfering buffers. With use of such membranes as a solid support, proteins are first reduced, then alkylated, and finally digested. Furthermore, there is an array of membranes types and cut-offs that make this method extremely versatile for proteomics. The FASP protocol offers a convenient way to handle the different steps of complicated workflows for proteome-wide quantification.

Received: April 6, 2020
Accepted: June 2, 2020
Published: June 2, 2020

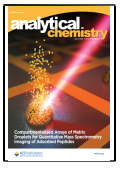

https://dx.doi.org/10.1021/acs.analchem.0c01470
Anal. Chem. 2020, 92, 9164−9171

In the present work, ultrasonic energy is introduced as a tool to speed up sample preparation in the standard FASP pipeline, and this new approach is named US-FASP. The ultrafiltration membrane in FASP acts as a proteomic reactor for detergent removal and buffer exchange, while ultrasonic energy is used to speed up chemical reactions and protein digestion. Overall, the treatment time is reduced from overnight to 2.5 h, which allows 36 samples to be processed simultaneously and facilitates high throughput sample preparation.

EXPERIMENTAL SECTION

***E. coli* Proteome.** *E. coli* samples were prepared using the ReadyPrepTM *E. coli* lysate sample from BioRad, following the manufacturers' instructions with minor modifications, as described in Supporting Information SI1. In some experiments to access the different methods' reproducibility, five different known concentrations of bovine serum albumin (BSA), β-lactoglobulin, α-casein, and α-lactalbumin were spiked to the *E. coli* proteome.

Mouse Liver and Brain Proteomes. Fresh frozen mouse liver and brain were obtained from Patricell Limited. Tissue proteome extraction was performed as described in SI2. Total protein content was determined by the Bradford protein assay.

Filter Aided Sample Preparation (FASP). The standard overnight digestion FASP, ON-FASP, depicted in Figure 1A, was used to process the *E. coli*, mouse brain, and liver proteome with a few minor modifications.[12−15] A total of 100 μg of *E. coli* protein was loaded in a membrane with a 10 000 molecular weight cutoff (MWCO). The same amounts of mouse brain and liver protein were loaded in a membrane with a 30 000 molecular weight cutoff (MWCO). The proteins present in the membrane were washed with 200 μL of 8 M urea, 25 mM AmBic solution and then centrifuged for 20 min at 14 000*g*. *E. coli* samples were reduced by adding 200 μL of 50 mM dithiothreitol (DTT) in 8 M urea and 25 mM AmBic and incubated for 60 min at 37 °C. Mouse brain and liver proteomes skipped the step of reduction as the lysis buffer had this already incorporated. A centrifugation of 20 min at 14 000*g* was then done, and the sample was alkylated during 45 min in the dark by the addition of 100 μL of 50 mM iodoacetamide (IAA) in 8 M urea and 25 mM AmBic solution. Subsequently, a centrifugation of 20 min at 14 000*g* was processed, and then the sample was washed twice with 200 μL of 25 mM AmBic. Finally, protein digestion was initiated by the addition of 100 μL of 1:30 trypsin in 12.5 mM AmBic solution. Protein digestion was proceeded overnight (approximately 16 h) at 37 °C, and then the peptides were collected by 20 min of centrifugation at 14 000*g*. To ensure that all of the peptides were extracted, 100 μL of 3% (v/v) acetonitrile and 0.1% (v/v) formic acid were added followed by a centrifugation of 20 min at 14 000*g*. This previous step was repeated one more time, and then the peptides were transferred to a 500 μL microtube, dried, and stored at −20 °C until further peptide quantification (SI3) and analysis by Nano-LC−MS/MS (SI4).

Ultrasonic-Based Filter Aided Sample Preparation (US-FASP). The US-FASP depicted in Figure 1A was used to process the protein *E. coli*, mouse brain, and mouse liver proteome and compared to the standard FASP described above. The same workflow, including cleaning steps, as described before, was used; however, ultrasound energy was applied to speed up the reduction, alkylation, and digestion steps. Briefly, the proteins were reduced by adding 200 μL of

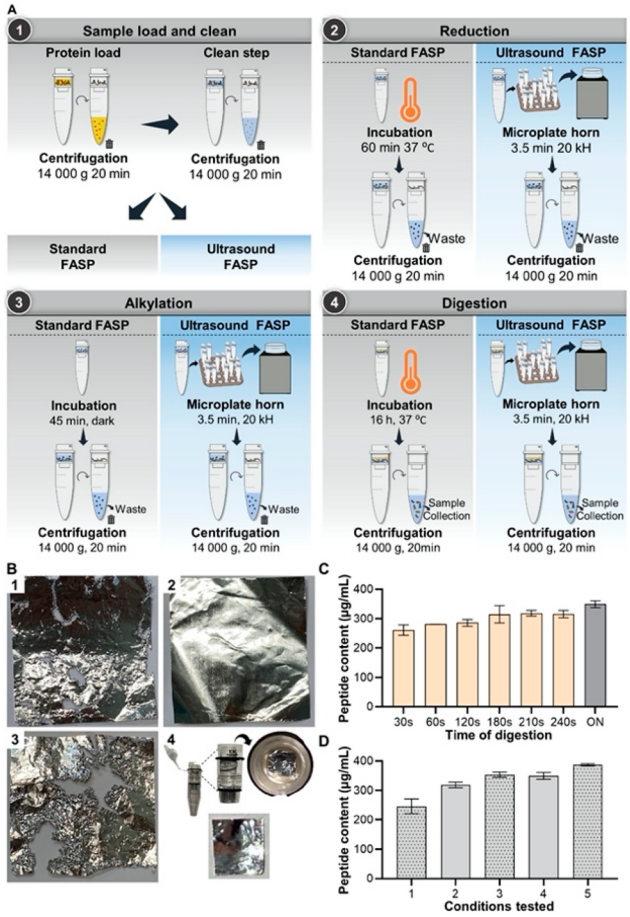

Figure 1. Ultrasonic-based filter aided sample preparation workflow and optimization. (A) Different methods, standard overnight digestion FASP (ON-FASP) and ultrasound FASP (US-FASP), were used to process *E. coli*, mouse brain, and liver proteomes. Ultrasound energy was used to speed up the reduction, alkylation, and digestion FASP steps. (B) Effect of ultrasound energy in 5 cm × 5 cm aluminum foils. (1) 30 s ultrasonic time, UT, in an ultrasound bath at 100% ultrasonic amplitude, UA, and 35 kHz ultrasonic frequency, UF. (2) 30 s UT in an ultrasound bath at 100% UA and 130 kHz UF. (3) 30 s UT in an ultrasonic microplate horn assembly at 25% UA and 20 kHz UF. (4) 5.25 min UT in an ultrasonic microplate horn assembly at 25% UA and 20 kHz UF (0.5 cm × 0.5 cm aluminum foil inside the FASP tube). (C) Digestion time optimization. Different total elapsed ultrasound digestion times (30, 60, 180, 210, and 240 s) were accessed using the ultrasonic microplate horn assembly at 25% UA and 20 kHz UF and compared to the ON-FASP. (D) Ultrasound in the reduction, alkylation, and digestion steps. Bars with gray color with and without dots represent different batches of *E. coli*. Different conditions using the ultrasonic microplate horn assembly were done (1, no reduction and alkylation step, use of ultrasound energy in the digestion; 2, standard alkylation step and use of ultrasound energy in the reduction and digestion step; 3, use of ultrasound in the reduction, alkylation, and digestion step) and compared to the ON-FASP (4, 5).

50 mM dithiothreitol (DTT) prepared in 8 M urea and 25 mM AmBic. Tissue samples skipped the step of reduction as this was already done during the tissue homogenization using the lysis buffer. Ultrasound energy was then applied using the ultrasonic microplate horn assembly for 5.25 min (7 cycles: 30 s on and 15 s off UT, 25% UA, 20 kHz UF). Afterward, centrifugation for 20 min at 14 000*g* was done, followed by protein alkylation by the addition of 100 μL of 50 mM

https://dx.doi.org/10.1021/acs.analchem.0c01470
Anal. Chem. 2020, 92, 9164−9171

iodoacetamide (IAA) prepared in 8 M urea and 25 mM AmBic solution. The alkylation step was sped up using the ultrasonic microplate horn assembly during 5.25 min (7 cycles: 30 s on and 15 s off UT, 25% UA, 20 kHz UF). Finally, 100 μL of 1:30 trypsin in 12.5 mM AmBic solution was added, and the protein digestion was processed using the ultrasonic microplate horn assembly for 5.25 min (7 cycles: 30 s on and 15 s off UT, 25% UA, 20 kHz UF). Peptides were dried and stored at −20 °C until further peptide quantification (SI3) and analysis by Nano-LC−MS/MS (SI4).

Nano-LC−MS/MS. Analysis was carried out using an Ultimate 3000 nano LC system coupled to an Impact HD (Bruker Daltonics) with a CaptiveSpray nanoBooster using acetonitrile as the dopant. Further details are provided in SI4. The mass spectrometry proteomics data have been deposited to the ProteomeXchange Consortium[27] via the PRIDE[28] partner repository with the data set identifier PXD018360.

Label-Free Protein Quantification and Statistical Analysis. Relative label-free quantification was carried out using MaxQuant software V1.6.10.43. All raw files were processed in a single run with default parameters.[16,17] Database searches were performed using the Andromeda search engine with the UniProt - Proteome_UP000000625, which contains proteins from *E. coli* and the sequences from the spiked proteins that were added to the fasta file.[18] Data processing was performed using Perseus (version 1.6.5.0) with default settings.[19] Protein group LFQ intensities were log 2-transformed, and the quantitative profiles were filtered for missing values with the following settings: min valid percentage of 70% in at least one group and values greater than 0. To overcome the obstacle of missing LFQ values, missing values were imputed using the parameters, with = 0.5 and down shift = 1.8.[19] Log ratios were calculated as the difference in average log 2 LFQ intensity values between the tested conditions (two-tailed, Student's *t* test, permutation-based FDR 0.05 and S0 of 0.1).

RESULTS AND DISCUSSION

Initial Considerations about Variables Affecting Ultrasonic Performance. Previous research performed in our laboratory has recently shown that the ultrasonic microplate horn assembly is the ultimate ultrasonic tool to speed up complex proteomics pipelines as 96 samples can be digested in 4 min, and volumes as low as 10 μL can be handled.[12] Thus, the analytical minimalism rules, as explained by Halls, are accomplished.[12,20] We have also shown that high intensity focused ultrasonic energy has two effects over enzymatic kinetics, first speeding up the kinetics and then, after 5 min, inactivating the enzyme.[21] Therefore, ultrasonic energy was not applied in this work for longer than 5 min. We have observed that ultrasonic amplitudes higher than 25% led to the rapid deterioration of the microplate horn assembly surface, but we demonstrated that for in-solution digestion of complex proteomes, such as *E. coli* lysates and tissue extracts, a 25% ultrasonic amplitude is adequate to speed the overnight proteome digestion process up to 4 min (intervals of 30 s on and 15 s off). Consequently, the ultrasonic amplitude chosen was 25%.[12]

Effect of Ultrasonic Frequency over the FASP Membrane. The implosion of ultrasonic nanobubbles generated by high-intensity ultrasound produced at frequencies between 20 and 40 kHz creates shock waves with disruptive effects.[22−24] However, at higher frequencies, this disruptive effect is less intense. Figure 1B1 and B2 shows two aluminum foils (5 × 5 cm) that were exposed to an ultrasonic field generated in an ultrasonic bath. Figure 1B1 clearly shows the disruptive effects over the aluminum foil of ultrasound generated at a frequency of 35 kHz, while Figure 1B2 shows that at a frequency of 130 kHz there is no disruption. The ultrasonic well plate works at a frequency of 20 kHz, and thus has a disruptive effect, which could potentially affect the membrane of the FASP tube. The difference in cavitation effects between the ultrasonic bath and the microplate horn is visualized in Figure 1B3, where it may be seen that the microplate horn's disruptive effect is more intense when the following conditions were used to deliver ultrasound: aluminum foil 5 × 5 cm, 30 s UT, 20 kHz UF, 25% UA. Therefore, the first task was to investigate the integrity of the FASP membrane. To this end, the effect of ultrasound energy over the FASP membrane was tested by introducing an aluminum foil in the FASP tube just over the membrane as depicted in Figure 1B4 (7 cycles: 30 s on and 15 s off UT, 25% UA, 20 kHz UF). It was found that the microtube walls have a protective effect, which diminishes the disruptive effects of ultrasound, as no disruption was observed either in the aluminum foil or in the FASP membrane (Figure SI5). This fact was later confirmed by the results obtained for protein identification and quantification as shown below. Moreover, no membrane polymers were observed in the mass spectra. However, during the first experiments with ultrasound, water was observed inside the FASP tubes after some tens of seconds of ultrasonication. To avoid this effect, it was necessary to develop a small modification on the FASP tube design consisting of the addition of two O-rings, as shown in video S1. Finally, once it was verified that (i) no degradation of the FASP membranes was observed under the effects of an ultrasonic field and that (ii) no water entered inside the FASP tube during ultrasonication, the next step was to assess the acceleration of the FASP protocol using ultrasonic energy.

Effect of Time of Ultrasonication in the FASP-Based Digestion Protocol. The workflow of complex proteomes can be divided into three main steps: reduction, to break disulfide bonds; alkylation, to inactivate sulfur groups, which thus hampers disulfide bonds from forming again; and finally protein cleavage using trypsin, also known as the protein digestion step. The latter is by far the step that consumes more time as it is generally done overnight (18 h). Therefore, our first efforts were oriented to shorten this step. To this end, a series of *E. coli* samples were digested overnight following the standard FASP. Other series of the same *E. coli* were also digested under the effects of an ultrasonic field during different times, comprising the range 0.5−4 min (reduction and alkylation were done with no US applied for both sets of samples). If the success of the digestion is measured as the concentration of peptides obtained with the overnight digestion protocol, Figure 1C shows that after 3 min of digestion under the effects of an ultrasonic field, the peptide content of the ultrasonically digested sample is 91 ± 8% of the sample digested overnight. Therefore, an ultrasonication time of 5.25 min was settled as optimum for the digestion protocol (7 cycles: 30 s on and 15 s off UT, 25% UA, 20 kHz UF).

Effect of Ultrasonication in Reduction and Alkylation Steps. Once it was verified that the overnight digestion process in the FASP membrane can be accelerated to 5.25 min, it was investigated if the alkylation and digestion processes could be also shortened. To this end, a series of experiments

https://dx.doi.org/10.1021/acs.analchem.0c01470
Anal. Chem. 2020, 92, 9164−9171

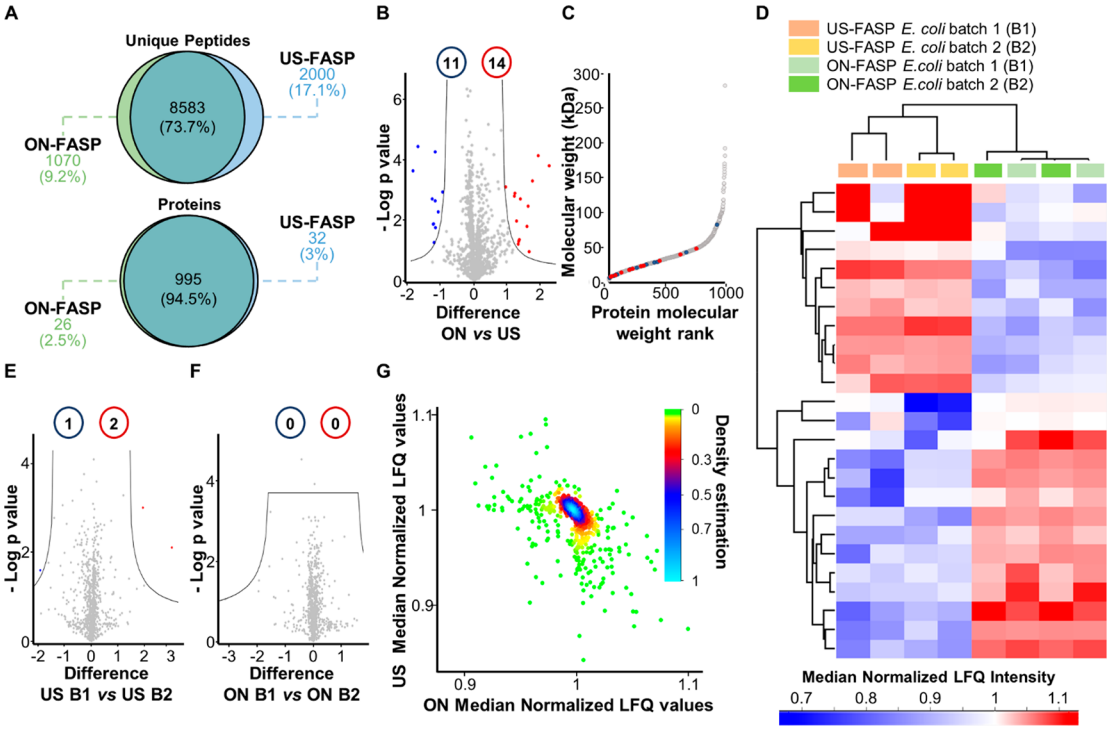

Figure 2. *E. coli* proteome digestion using the US-FASP and ON-FASP. (A) Venn diagram of the identified peptides and proteins in the US-FASP and ON-FASP. Different proteins identified in each method with a filter of 70% in at least one group. (B) Volcano plot showing the variation in protein levels in the comparison of ON-FASP versus US-FASP. Proteins were normalized by the median of each protein, and a two-tailed Student's *t* test (FDR 0.05 and S0 of 0.1, $n = 8$) was used for statistical analysis. Blue and red color dots represent the statistically significant proteins (numbers inside the colored circles), while the gray dots represent the nonstatistically significant proteins, respectively. (C) Protein molecular weight rank in the methods of digestion ON-FASP and US-FASP. (D) Hierarchal clustering with average linkage using the statically significant proteins (two-tailed Student's *t* test, FDR 0.05 and S0 of 0.1, $n = 8$). (E,F) Batch effect in each method. Protein levels were normalized by the median of each protein, and statistically significant changes were detected using a two-tailed Student's *t* test (FDR 0.05 and S0 of 0.1, $n = 4$). (G) Correlation plot and density from the comparison of ON-FASP versus US-FASP. Correlation plot of the proteins with median-based normalization shows a distribution centered around 1, which reflects a lower variation between the tested methods.

were designed in which *E. coli* extracts were submitted to reduction, alkylation, and digestion, with and without the effects of an ultrasonic field (7 cycles: 30 s on and 15 s off UT, 25% UA, 20 kHz UF). First, it was investigated whether the process could be done by applying ultrasound only in the digestion step, while skipping the alkylation and reduction steps. The results of this experiment are shown in Figure 1D1, and it may be seen that 60% of the expected peptide concentration is obtained. Next, we apply ultrasound only in the reduction and digestion steps, while skipping the application of ultrasound in the alkylation process. However, the results were not satisfactory as only 80% of the expected peptides were obtained (Figure 1D2). Finally, when all of the steps, reduction, alkylation, and digestion, were done under the effects of an ultrasonic field, the concentration of peptides was more than 90% of the expected amount (Figure 1D3). Thus, the set of experiments described above showed that ultrasonic energy conveniently speeds up each step of the proteomic workflow (Figure 1D4 and D5).

Finally, in further experiments, and as best conditions, for each step assessed (reduction, alkylation, and digestion), 5.25 min of ultrasonication time was applied in periods of 30 s followed by resting periods of 15 s seconds (total time of 5.25 min UT, with a 25% UA and at an UF of 20 kHz).

Mass Spectrometry Label Free-Based Protein Quantification: Ultrasonic-Based FASP versus Classic Overnight FASP. Figure 2 shows the comparison of ultrasonic-based FASP protocol, US-FASP, versus classic overnight FASP, ON-FASP, protocol using *E. coli* samples and label free-based mass spectrometry ($n = 2$ different batches for each protocol run in two different days, with two technical replicates each batch, resulting in a total of four samples for each method). The two conditions tested resulted in 11 653 unique peptides and 1053 proteins, Figure 2A. Of the unique peptides identified, 8583 (73.7%) were found common for both methods, from which (i) 7022 peptides (81.8%) had no missed cleavages, (ii) 1432 peptides (16.7%) had one missed cleavage, and (iii) 125 unique peptides (1.5%) had two missed cleavages. Of the 1053 identified proteins, 995 (94.5%) were found common for both methods, Figure 2A. The second step was to quantify differences in digestion efficiency across the detected proteome. These differences are shown in Figure 2B. This volcano plot shows that only 25 proteins are differentially digested, which represents 2% of the detected proteome (two-tailed Student's *t* test, FDR 0.05 and S0 of 0.1, $n = 8$). This result shows the similarity of both proteomic pipelines (Figure SI6). Furthermore, Figure 2C shows that the majority of the 2% of proteins found with different digestion efficiencies are of a molecular weight below 50 kDa. Interestingly, when these 25 proteins are used to generate a hierarchical clustering, Figure 2D, it becomes evident that such proteins are preferentially digested either by the US-FASP or by the ON-FASP. This observation is in agreement with the results reported previously.[9,12]

https://dx.doi.org/10.1021/acs.analchem.0c01470
Anal. Chem. 2020, 92, 9164−9171

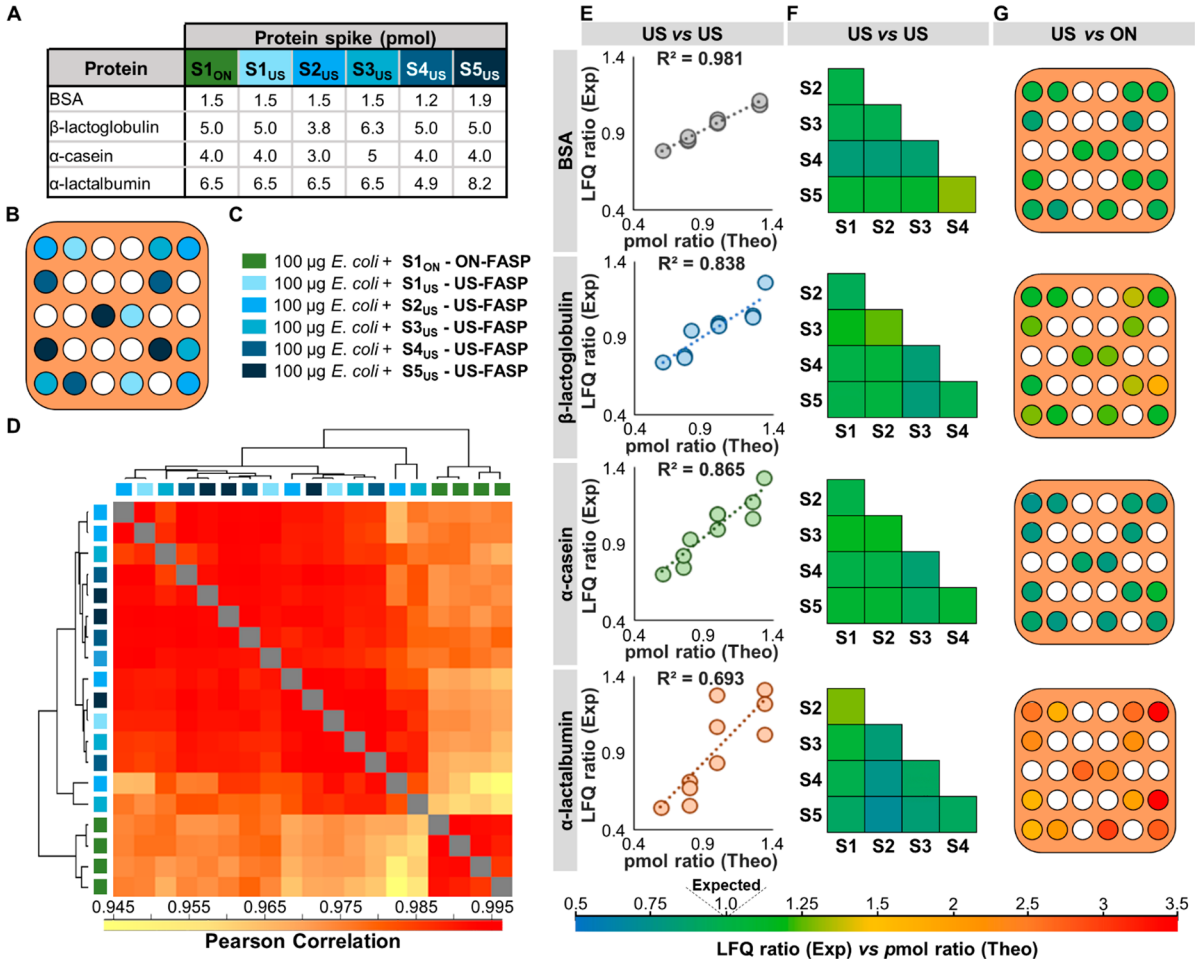

Figure 3. Ultrasonic space effectiveness in US-FASP. (A) Protein spikes and *E. coli* used in each condition. (B) Position of the different samples in the ultrasonication plate. (C) *E. coli* proteome and spiked proteins processed with ON-FASP and US-FASP. (D) Cluster by Pearson correlation of the *E. coli* samples with the different protein spikes using the ON-FASP and US-FASP. (E, F, and G) Comparison between the theoretical pmol ratio (theo) and the LFQ values obtained ratio (exp). The protein spikes were compared as follows: (E,F) US-FASP versus US-FASP and (G) US-FASP versus ON-FASP. The difference was obtained using formulas 1−5.

The reproducibility for each method was assessed as the difference between two batches of the same sample done in different days, and it is shown in Figure 2E and F. These volcano plots show that the interdaily variability of both methods is negligible (two-tailed Student's *t* test, FDR 0.05 and S0 of 0.1, $n = 4$ each method). When the 1053 protein LFQ values obtained after finishing each experimental pipeline are compared using the median-based normalization, the distribution is centered around 1, as shown in Figure 2G, which further reflects the few differences between both US- and ON-sample treatments.

Performance of Ultrasonic-Based FASP. To verify the homogeneity of the ultrasonic effects inside the microplate horn, *E. coli* samples were distributed randomly and were spiked at different levels with four proteins, as depicted in Figure 3A and B. The samples then were overnight or ultrasonically digested as depicted in Figure 3C. When the complete set of *E. coli* proteins of each sample is identified and quantified and then used to cluster the samples, the reproducibility as expressed by the Pearson correlation value is higher than 0.985 (Figure 3D), which shows that the digestion of the *E. coli* proteomes is done with the same efficiency in all of the positions and thus concludes that the effects of the ultrasound energy are homogeneously distributed in the entire microplate horn. Moreover, when the ultrasonic treated samples are compared to the overnight treated ones (Figure 1D), the Pearson correlations are higher than 0.945, which again indicates that for a few proteins both methods perform slightly different but for the majority both perform equally.

Ultrasonic-Based FASP Label-Free Quantification of a Set of Spiked Proteins in *E. coli* Samples. To get a deeper insight into the potentialities of the proposed US-FASP method, *E. coli* samples were spiked with four known proteins, BSA, *β*-lactoglobulin, *α*-casein, and *α*-lactalbumin. The known protein amount ratios (Figure 3A) between samples were compared to their respective mass spectrometer signal ratios (LFQs ratio) using the formulas:

$$\text{pmol ratio (theo)} = \frac{\text{Spike}_{Sx}}{\text{Spike}_{Sy}} \quad (1)$$

$$\text{LFQ ratio (exp)} = \frac{\bar{X}\ \text{LFQ}_{Sx}}{\bar{X}\ \text{LFQ}_{Sy}} \quad (2)$$

where x and y can be samples S1, S2, S3, S4, or S5, Spike_{Sx} and Spike_{Sy} refer to the spikes added to the samples as they are presented in Figure 3A, and LFQ_{Sx} and LFQ_{Sy} refer to the

https://dx.doi.org/10.1021/acs.analchem.0c01470
Anal. Chem. 2020, 92, 9164−9171

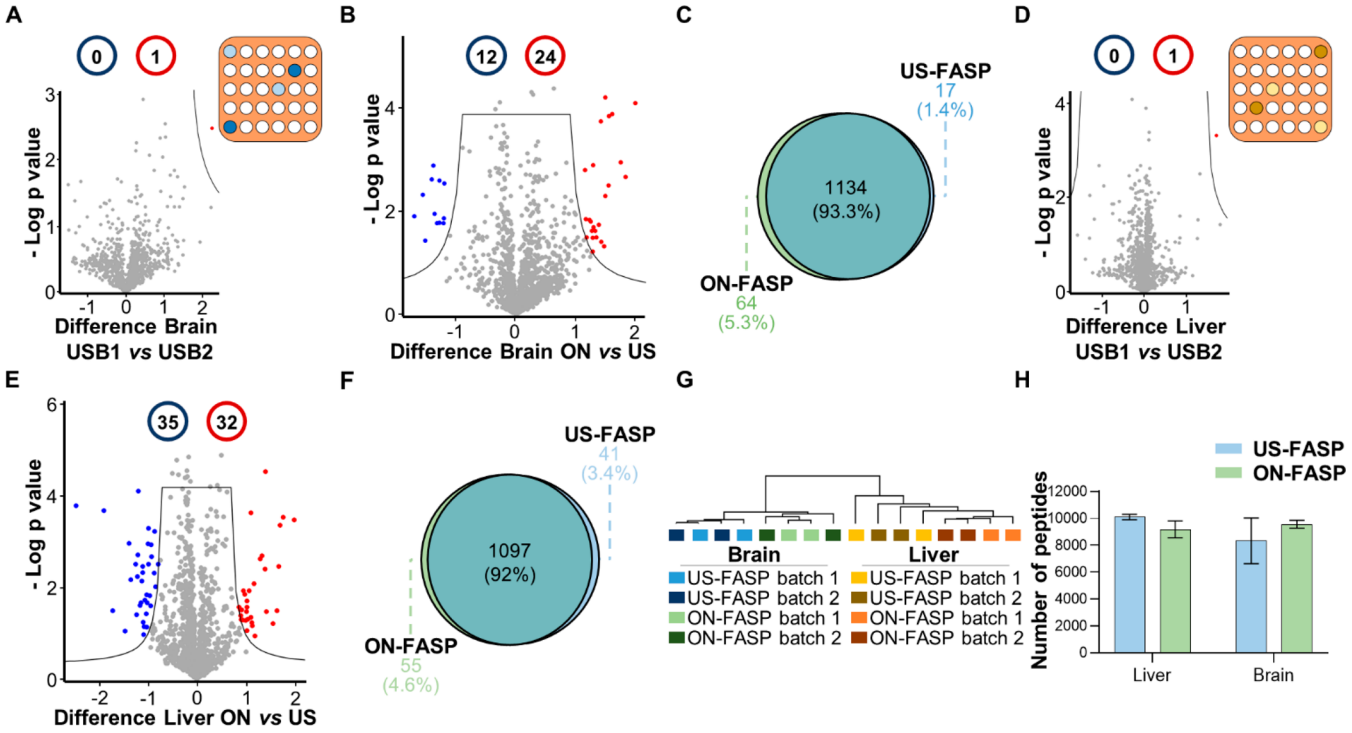

Figure 4. Mouse liver and brain proteome digestion using the US-FASP. (A−C) Quantitative proteomics analysis using the US-FASP and ON-FASP methods in brain mouse tissues. (D−F) Quantitative proteomics analysis using the US-FASP and ON-FASP methods in liver mouse tissues. (A and D) Batch and plate position effect in the US-FASP method. Volcano plot comparing each batch of tissue with random position in the ultrasonication plate. Protein levels were normalized by the median of each protein, and the different quantified proteins were obtained using a two-tailed Student's *t* test (FDR 0.05 and S0 of 0.1, $n = 4$). Blue and red color dots represent the statistically significant proteins (numbers inside the colored circles), while the gray dots represent the nonstatistically significant proteins, respectively. (B and E) Protein quantitative levels comparison between the US-FASP and ON-FASP methods. Volcano plot comparing the protein levels in each method. Protein levels were normalized by the median of each protein, and the different quantified proteins were obtained using a two-tailed Student's *t* test (FDR 0.05 and S0 of 0.1, $n = 8$). (C and F) Venn diagram with the proteins identified by US-FASP and ON-FASP method. Different proteins identified in each method with a filter of 70% presence in at least one group. (G) Cluster of the mouse brain and liver tissues processed by ON-FASP and US-FASP. Protein identified with a filter of 70% presence in at least one group was normalized by Z-score and a multisample test; ANOVA (FDR 0.05, $n = 16$) were plotted in a hierarchal clustering. (H) Number of peptides identified in each tissue type with the different FASP methods used. ON-FASP method is represented by the green color bars and US-FASP by the blue color bars.

respective mass spectrometry data of samples *x* and *y*. The quantification results are depicted in Figure 3E, where it may be seen that for proteins BSA, *β*-lactoglobulin, and *α*-casein the spiked ratios match close to the LFQ ratios, which is reflected in the regression coefficients close to 1. For the case of *α*-lactalbumin, the match is worst, with a regression coefficient of ca. 0.7.

In an ideal situation, where the proteins are efficiently digested and where the LFQs are proportional to the protein concentration, the ratio using the formula

$$\text{ratio} = \frac{\text{LFQ ratio (exp)}}{\text{pmol ratio (theo)}} \tag{3}$$

should be 1. When this ratio is calculated for the different positions inside the microplate horn, as shown in Figure 3F, it can be seen that the effects of ultrasonic energy are homogeneously distributed all over the surface, with the best results being obtained for BSA and the worst for *α*-lactalbumin. Thus, for BSA protein, the differences between the pmol ratios and the LFQs ratios were up to 6% ($n = 10$, range 1−13.5%), for the *β*-lactoglobulin they were 20% ($n = 10$, range 15−22%), and for *α*-casein they were 15% ($n = 10$, range 6−19%). For *α*-lactalbumin, the results were the worst, and the difference was 56% ($n = 10$, range 35−91%).

Ultrasonic-Based FASP versus Classic FASP Label-Free Quantification of a Set of Spiked Proteins in *E. coli* Samples. The final insight was done by comparing the values of the US-FASP versus ON-FASP for the four spiked proteins as follows:

$$\text{pmol ratio (theo)} = \frac{\text{Spike}_{\text{S1 ON}}}{\text{Spike}_{\text{S}x\text{ US}}} \tag{4}$$

$$\text{LFQ ratio (exp)} = \frac{\bar{X}\ \text{LFQ}_{\text{S1 ON}}}{\text{LFQ}_{\text{S}x\text{ US}}} \tag{5}$$

where $\text{Spike}_{\text{S}x\text{ US}}$ can be ultrasonic treated samples S1, S2, S3, S4, or S5, $\text{Spike}_{\text{S1 ON}}$ refers to the sample treated overnight (see Figure 3C), $\text{LFQ}_{\text{S}x\text{ US}}$ refers to the mass spectrometry data of ultrasonic treated samples S1, S2, S3, S4, or S5, and $\text{LFQ}_{\text{S1 ON}}$ refers to the mass spectrometry data obtained for the sample treated overnight.

The ratio, using formula 3, was then calculated. This ratio should ideally be 1. It can be seen in Figure 3G that proteins BSA, *β*-lactoglobulin, and *α*-casein are digested at the same level using either the ultrasonic or the overnight method. For the case of the *α*-lactalbumin, the digestion was better for the overnight method, almost 1.5 times better.

https://dx.doi.org/10.1021/acs.analchem.0c01470
Anal. Chem. 2020, 92, 9164−9171

Application to Brain and Liver Tissue Samples. The optimum sample treatment conditions were also applied to tissue samples. To this end, brain and liver tissue samples were submitted to the protein extraction explained in the Experimental Section, and, of each protein tissue extract, four subsamples were made. These subsamples were divided into two groups of two samples each. Samples were digested with the optimized conditions in different positions inside the microplate horn in different days as depicted in Figure 1. The results are shown in Figure 4. The first interesting fact is that no differences were found neither in the number of proteins nor in their quantification values when the analysis was done on different days (Figure 4A and D). Moreover, the same data also reflect that the position where the digestion is done inside the microplate horn does not affect the digestion efficiency (Figure 4B and E). Furthermore, the number of common proteins identified for each tissue type was almost the same regardless of the sample treatment used, 1134 (93.3%) for the brain tissue and 1097 (92%) for the liver tissue (Figure 4 C and F, respectively). In addition, the number of peptides identified was also similar for each method and each tissue type (Figure 4H). Finally, the data obtained also allow a nice classification of both tissues (Figure 4G).

CONCLUSION

A novel ultrasonic-assisted filter aided sample preparation protocol has been developed for large-scale proteomics approaches, which allows high sample throughput and reduces the treatment time from 18 to 2.5 h for a total of 36 samples. The method is scalable to 96 samples using 96-well plates and virtually applicable to similar digestion platforms such as S-Trap.[25] We foresee this method as the universal one for proteomics pipelines as it paves the way to clinical proteomics in hospitals because it is of easy handling as the operator needs no special skills. Also, this method matches perfectly the new high-resolution mass spectrometers that allow fast chromatographic runs in 15 min, which thus allows one to measure the proteome of about 100 samples a day per spectrometer. Further, shortening of the sample processing time can be achieved by skipping the cysteine alkylation step.[26]

ASSOCIATED CONTENT

Supporting Information

The Supporting Information is available free of charge at https://pubs.acs.org/doi/10.1021/acs.analchem.0c01470.

Appendix A: Supplementary data containing the reagents and apparatus used, extended experimental section (SI1−4), optical microscopy FASP membrane images (Figure SI5), hierarchal clustering of the *E. coli* proteome processed with US-FASP and ON-FASP (Figure SI6), and a custom-built wood plate vivacon support floater (Figure SI7) (PDF)

Video S1: Video showing the digestion step in the US-FASP digestion method (MP4)

AUTHOR INFORMATION

Corresponding Author

Hugo M. Santos − *BIOSCOPE Research Group, LAQV-REQUIMTE, Department of Chemistry, Faculty of Science and Technology, Universidade NOVA de Lisboa, Caparica 2829-516, Portugal; PROTEOMASS Scientific Society, Madan Parque, Caparica 2825-182, Portugal; Department of Pathology, University of Pittsburgh Medical Center, Pittsburgh, Pennsylvania 15213, United States;* orcid.org/0000-0002-6032-8679; Phone: +351 934 432 320; Email: hmsantos@fct.unl.pt

Authors

Luís B. Carvalho − *BIOSCOPE Research Group, LAQV-REQUIMTE, Department of Chemistry, Faculty of Science and Technology, Universidade NOVA de Lisboa, Caparica 2829-516, Portugal; PROTEOMASS Scientific Society, Madan Parque, Caparica 2825-182, Portugal;* orcid.org/0000-0002-3761-8512

José-Luis Capelo-Martínez − *BIOSCOPE Research Group, LAQV-REQUIMTE, Department of Chemistry, Faculty of Science and Technology, Universidade NOVA de Lisboa, Caparica 2829-516, Portugal; PROTEOMASS Scientific Society, Madan Parque, Caparica 2825-182, Portugal;* orcid.org/0000-0001-6276-8507

Carlos Lodeiro − *BIOSCOPE Research Group, LAQV-REQUIMTE, Department of Chemistry, Faculty of Science and Technology, Universidade NOVA de Lisboa, Caparica 2829-516, Portugal; PROTEOMASS Scientific Society, Madan Parque, Caparica 2825-182, Portugal;* orcid.org/0000-0001-5582-5446

Jacek R. Wiśniewski − *Biochemical Proteomics Group, Department of Proteomics and Signal Transduction, Max-Planck-Institute of Biochemistry, Martinsried D-82152, Germany;* orcid.org/0000-0002-8452-5095

Complete contact information is available at: https://pubs.acs.org/10.1021/acs.analchem.0c01470

Author Contributions

J.-L.C.-M., C.L., and H.M.S. designed the experimental work and provided financial support. L.B.C. performed the laboratorial work under the supervision of H.M.S. J.-L.C.-M. and H.M.S. drafted the manuscript. J.-L.C.-M., C.L., J.R.W., and H.M.S. revisited the drafted version, corrected it, and made valuable suggestions.

Notes

The authors declare no competing financial interest.

ACKNOWLEDGMENTS

PROTEOMASS Scientific Society is acknowledged for the funding provided to the Laboratory for Biological Mass Spectrometry − Isabel Moura. We acknowledge the funding provided by the Associate Laboratory for Green Chemistry LAQV, which is financed by national funds from FCT/MEC (UID/QUI/50006/2019). H.M.S. and L.B.C. acknowledge the funding provided by FCT/MEC within the framework of the FCT Investigator Program (IF/00007/2015) and the Ph.D. grant (SFRH/BD/144222/2019), respectively. We acknowledge Eng. F. Silvestre from FCT FabLab (powered by USA Embassy) for his help in the manufacturing of the wood plate vivacon support floater, Figure S7.

REFERENCES

(1) López-Ferrer, D.; Cañas, B.; Vázquez, J.; Lodeiro, C.; Rial-Otero, R.; Moura, I.; Capelo, J. L. *TrAC, Trends Anal. Chem.* **2006**, *25* (10), 996−1005.

(2) Capelo, J. L.; Carreira, R.; Diniz, M.; Fernandes, L.; Galesio, M.; Lodeiro, C.; Santos, H. M.; Vale, G. *Anal. Chim. Acta* **2009**, *650* (2), 151−159.

(3) Shen, X.; Sun, L. *Proteomics* **2018**, *18* (9), 1700432.

(4) López-Ferrer, D.; Capelo, J. L.; Vázquez, J. *J. Proteome Res.* **2005**, *4* (5), 1569−1574.
(5) Rial-Otero, R.; Carreira, R. J.; Cordeiro, F. M.; Moro, A. J.; Fernandes, L.; Moura, I.; Capelo, J. L. *J. Proteome Res.* **2007**, *6* (2), 909−912.
(6) Santos, H. M.; Rial-Otero, R.; Fernandes, L.; Vale, G.; Rivas, M. G.; Moura, I.; Capelo, J. L. *J. Proteome Res.* **2007**, *6* (9), 3393−3399.
(7) Galesio, M.; Vieira, D. V.; Rial-Otero, R.; Lodeiro, C.; Moura, I.; Capelo, J. L. *J. Proteome Res.* **2008**, *7* (5), 2097−2106.
(8) Santos, H. M.; Mota, C.; Lodeiro, C.; Moura, I.; Isaac, I.; Capelo, J. L. *Talanta* **2008**, *77* (2), 870−875.
(9) Jesus, J. R.; Santos, H. M.; López-Fernández, H.; Lodeiro, C.; Arruda, M. A. Z.; Capelo, J. L. *Talanta* **2018**, *178*, 864−869.
(10) Martins, G.; Fernández-Lodeiro, J.; Djafari, J.; Lodeiro, C.; Capelo, J. L.; Santos, H. M. *Talanta* **2019**, *196*, 262−270.
(11) Jorge, S.; Capelo, J. L.; LaFramboise, W.; Dhir, R.; Lodeiro, C.; Santos, H. M. *J. Proteome Res.* **2019**, *18* (7), 2979−2986.
(12) Jorge, S.; Araújo, J. E.; Pimentel-Santos, F. M.; Branco, J. C.; Santos, H. M.; Lodeiro, C.; Capelo, J. L. *Talanta* **2018**, *178*, 1067−1076.
(13) Wiśniewski, J. R.; Zougman, A.; Nagaraj, N.; Mann, M. *Nat. Methods* **2009**, *6* (5), 359−362.
(14) Wiśniewski, J. R. *Anal. Chim. Acta* **2019**, *1090*, 23−30.
(15) Carvalho, L. B.; Capelo-Martínez, J. L.; Lodeiro, C.; Wiśniewski, J. R.; Santos, H. M. *Anal. Chim. Acta* **2019**, *1076*, 82−90.
(16) Cox, J.; Mann, M. *Nat. Biotechnol.* **2008**, *26* (12), 1367−1372.
(17) Tyanova, S.; Temu, T.; Carlson, A.; Sinitcyn, P.; Mann, M.; Cox, J. *Proteomics* **2015**, *15* (8), 1453−1456.
(18) Cox, J.; Neuhauser, N.; Michalski, A.; Scheltema, R. A.; Olsen, J. V.; Mann, M. *J. Proteome Res.* **2011**, *10* (4), 1794−1805.
(19) Tyanova, S.; Temu, T.; Sinitcyn, P.; Carlson, A.; Hein, M. Y.; Geiger, T.; Mann, M.; Cox, J. The Perseus computational platform for comprehensive analysis of (prote)omics data. *Nature Methods*; Nature Publishing Group: New York, 2016; pp 731−740.
(20) Halls, D. J. *J. Anal. At. Spectrom.* **1995**, *10* (3), 169−175.
(21) Galesio, M.; Loureno, J.; Madeira, D.; Diniz, M.; Capelo, J. L. *J. Mol. Catal. B: Enzym.* **2012**, *74* (1−2), 9−15.
(22) Suslick, K. S.; Nyborg, W. L. *J. Acoust. Soc. Am.* **1990**, *87* (2), 919−920.
(23) Mason, T. J. *Dev. Cardiovasc. Med.* **1996**, *178*, 25−54.
(24) Capelo-Martínez, J.-L. *Ultrasound in Chemistry: Analytical Applications*; Wiley-VCH: New York, 2009.
(25) Ludwig, K. R.; Schroll, M. M.; Hummon, A. B. *J. Proteome Res.* **2018**, *17*, 2480−2490.
(26) Wiśniewski, J. R.; Zettl, K.; Pilch, M.; Rysiewicz, B.; Sadok, I. *Anal. Chim. Acta* **2020**, *1100*, 131−137.
(27) Deutsch, E. W.; Bandeira, N.; Sharma, V.; Perez-Riverol, Y.; Carver, J. J.; Kundu, D. J.; García-Seisdedos, D.; Jarnuczak, A. F.; Hewapathirana, S.; Pullman, B. S.; Wertz, J.; Sun, Z.; Kawano, S.; Okuda, S.; Watanabe, Y.; Hermjakob, H.; MacLean, B.; MacCoss, M. J.; Zhu, Y.; Ishihama, Y.; Vizcaíno, J. A. *Nucleic Acids Res.* **2019**, *48* (D1), D1145−D1152.
(28) Perez-Riverol, Y.; Csordas, A.; Bai, J.; Bernal-Llinares, M.; Hewapathirana, S.; Kundu, D. J.; Inuganti, A.; Griss, J.; Mayer, G.; Eisenacher, M.; Pérez, E.; Uszkoreit, J.; Pfeuffer, J.; Sachsenberg, T.; Yilmaz, S.; Tiwary, S.; Cox, J.; Audain, E.; Walzer, M.; Jarnuczak, A. F.; Ternent, T.; Brazma, A.; Vizcaíno, J. A. *Nucleic Acids Res.* **2019**, *47* (D1), D442−D450.

https://dx.doi.org/10.1021/acs.analchem.0c01470
Anal. Chem. 2020, 92, 9164−9171